Open Journal of Mathematical Sciences

PSR Press

Article

Bayesian and frequentist inference for the Secant–Weibull ACD model with calendar effects

Omer Mohamed Egeh[1,2,*], Philip Odhiambo Ngare[3], Jane Akinyi Aduda[4], Christophe Chesneau[5] and Abdisalam Hassan Muse[6]

1 Department of Mathematics (Statistics Option), Pan African University, Institute for Basic Sciences, Technology, and Innovation (PAUSTI), Nairobi, Kenya
2 Department of Statistics, Amoud University, Borama, Somalia
3 Department of Financial Mathematics and Actuarial Science, University of Nairobi, Kenya
4 Department of Statistics and Actuarial Sciences, Jomo Kenyatta University of Agriculture and Technology (JKUAT), Nairobi, Kenya
5 Department of Mathematics, LMNO, CNRS-Université de Caen, Campus II, Science 3, 14032 Caen, France
6 Director, Research and Innovation Centre, Amoud University, Borama, Somalia
* Correspondence: omar.m.e@amoud.edu.so

Received: 23 Feb 2026; Revised: 26 Mar 2026; Accepted: 15 Apr 2026; Published: 06 May 2026

Abstract: This study introduces the Secant–Weibull Autoregressive Conditional Duration (SW–ACD) model and its extension with exogenous calendar effects (SW–ACD–X) . The primary innovation is the integration of the Secant-Weibull distribution as the innovation law, which allows the framework to capture non-monotonic intensity shapes, such as unimodal and bathtub patterns, that are typically inaccessible to standard monotonic models. A significant methodological contribution is the SW–ACD–X model, which endogenously incorporates intraday seasonality into the conditional mean equation. This joint estimation strategy provides an integrated alternative to traditional two-step pre-filtering by simultaneously capturing the interaction between deterministic diurnal patterns and stochastic duration clustering. The numerical properties of the proposed models are assessed through Monte Carlo simulations, which demonstrate asymptotic consistency while highlighting inherent identification challenges in small-sample regimes. Model estimation is implemented using a dual approach: Frequentist Maximum Likelihood and Bayesian Hamiltonian Monte Carlo (HMC) via the No-U-Turn Sampler (NUTS) in `RStan`. Empirical application to high-frequency IBM transaction data shows that the SW–ACD–X exhibits promising fit advantages over established benchmarks, including the W–ACD–X, LW–ACD–X, G-ACD-X , and Lomax–ACD–X models. Comprehensive model selection based on AIC, BIC, WAIC, and LOOIC confirms that the proposed model is a robust tool for analyzing market microstructure, liquidity dynamics, and the complex patterns of high-frequency durations.

Keywords: Secant–Weibull, SW–ACD–X, high-frequency data, Bayesian inference, HMC–NUTS, calendar effects, WAIC, LOOIC

MSC: Primary 62M10; Secondary 91G70.

1. Introduction

In high-frequency financial markets, transaction durations provide essential information on market microstructure, liquidity formation, and risk transmission mechanisms [1]. Duration data are strictly positive and typically exhibit pronounced right skewness, heavy tails, and temporal dependence, with clustering behavior analogous to volatility clustering in asset returns [2]. These characteristics pose substantial challenges for classical duration models.

The Autoregressive Conditional Duration (ACD) model introduced by [3] addresses such dependence by decomposing observed durations into a conditional mean component and a stochastic innovation. Within this framework, the choice of the innovation distribution is critical, as it governs the shape of the conditional intensity function and the model's capacity to capture persistence and tail behavior [4]. Although several extensions have been proposed, including the Weibull, Log-Weibull, and Generalized Gamma ACD models

[5,6], most of these specifications impose monotonic intensity structures and therefore failure to accommodate empirically observed non-monotonic patterns such as unimodal or bathtub-shaped intensities [7].

An additional challenge in ACD modeling concerns the treatment of intraday seasonality. Many existing studies adopt two-step pre-filtering procedures to remove calendar effects prior to model estimation [8]. This strategy implicitly assumes independence between deterministic intraday patterns and stochastic duration dynamics. In high-frequency financial markets, however, these components are often interrelated, and separating them may result in biased parameter estimates and distorted statistical inference [9].

Recent developments in distribution theory indicate that secant-based generators provide a flexible and analytically tractable framework for modeling heavy-tailed data with complex conditional intensity shape. In particular, the Secant-*G* family proposed by [10] allows for rich non-monotonic intensity structures. Despite its flexibility, this class of distributions has not yet been explored within the ACD modeling framework.

Motivated by these considerations, this study proposes the Secant-Weibull Autoregressive Conditional Duration model with calendar effects (SW-ACD-X). The model employs the Secant-Weibull distribution as a flexible innovation specification and incorporates calendar effects directly into the conditional mean equation. This joint modeling strategy captures intraday seasonality and stochastic duration dynamics simultaneously, thereby reducing the biases associated with conventional two-step approaches.

2. Methodology

The following section establishes an ACD framework that incorporates calendar effects and presents the Secant-Weibull distribution as a flexible innovation specification. Parameter estimation is performed using a dual approach: Frequentist Maximum Likelihood Estimation (MLE) and Bayesian inference via RStan. The proposed framework is subsequently verified through empirical analysis and Monte Carlo simulation studies.

2.1. Model formulation

2.1.1. ACD model

To describe the time interval between two consecutive events occurring at times t_i and t_{i-1}, the duration is defined as $x_i = t_i - t_{i-1}$. Following the seminal Autoregressive Conditional Duration (ACD) framework of [3], each observed duration x_i is decomposed into a predictable conditional mean component ψ_i and a stochastic innovation ϵ_i, such that

$$x_i = \psi_i \epsilon_i, \qquad \epsilon_i \sim \text{i.i.d. } g(\epsilon; \boldsymbol{\theta}), \tag{1}$$

where $g(\cdot)$ is the probability density function of the innovation term, and $E[\epsilon_i] = 1$.

A primary limitation of traditional ACD specifications is the need for external pre-filtering to remove diurnal seasonality. To address this issue, the SW–ACD–X(1,1) model incorporates calendar effects directly into the conditional mean by including a vector of indicator variables $Z_{i-1,1}$ within the recursion as follows:

$$\psi_i = \omega + \alpha_1 x_{i-1} + \beta_1 \psi_{i-1} + \gamma_1 Z_{i-1,1}. \tag{2}$$

By estimating the calendar-effect coefficients $\boldsymbol{\gamma_1}$ jointly with the Autoregressive parameters α_1 and β_1, the proposed model captures the interaction between deterministic intraday patterns and stochastic duration clustering.

2.1.2. Baseline distribution (Secant-Weibull)

The Secant-Weibull (SW) distribution is a new and flexible two-parameter model developed from the Secant-G family [10]. It is obtained by applying a trigonometric secant transformation to the CDF of the classical Weibull distribution. This structure gives the SW distribution strong adaptability, enabling it to capture features often observed in financial duration data, such as skewness, heavy tails (leptokurtosis), and non-monotonic conditional intensity patterns. A major advantage of the SW distribution is its simplicity: with only two parameters, it can represent all six well-known intensity shapes including hump-shaped and bathtub-shaped that are difficult to capture with the standard Weibull or more complex models like the Log Weibull distribution. The SW distribution is a good option for modelling improvements in ACD models

because of the balance between flexibility and symmetry. We use the CDF of Weibull distribution as the baseline,given by

$$G(x) = 1 - e^{-(x/\lambda)^k}, \quad x \geq 0,\ \lambda > 0,\ k > 0.$$

By applying the transformation defined in the preceding equation, we derive the Secant-Weibull distribution,with the CDF given by

$$F(x) = \sec\left(\frac{\pi}{3}\left(1 - e^{-(x/\lambda)^k}\right)\right) - 1. \tag{3}$$

The PDF of SW distribution is given by

$$f(x) = \frac{\pi k}{3\lambda}\left(\frac{x}{\lambda}\right)^{k-1} e^{-(x/\lambda)^k} \sec\left[\frac{\pi}{3}\left(1 - e^{-(x/\lambda)^k}\right)\right] \tan\left[\frac{\pi}{3}\left(1 - e^{-(x/\lambda)^k}\right)\right]. \tag{4}$$

The conditional intensity function is given by

$$h(x) = \frac{f(x)}{1 - F(x)}.$$

Substituting the PDF $f(x)$ and duration function $1 - F(x)$, we get the following conditional intensity function:

$$h(x) = \frac{\frac{\pi k}{3\lambda}\left(\frac{x}{\lambda}\right)^{k-1} e^{-(x/\lambda)^k} \cdot \sec\left(\frac{\pi}{3}\left(1 - e^{-(x/\lambda)^k}\right)\right) \tan\left(\frac{\pi}{3}\left(1 - e^{-(x/\lambda)^k}\right)\right)}{2 - \sec\left(\frac{\pi}{3}\left(1 - e^{-(x/\lambda)^k}\right)\right)}.$$

The secant and tangent transformations in the Secant-Weibull distribution allow for non-monotonic, heavy-tailed shapes of conditional intensity. This flexibility improves model fit for financial durations that often display overdispersion, extreme events, and volatility clustering.

Quantile Function. The Quantile function is essential for Monte Carlo simulations and is derived by inverting the CDF:

$$Q(u) = \lambda\left[-\ln\left(1 - \frac{3}{\pi}\operatorname{arcsec}(u+1)\right)\right]^{1/k}, \tag{5}$$

where $u \in (0,1)$.This allows for the direct generation of Secant-Weibull random variables.

2.1.3. Shapes of the Secant-Weibull distribution

In this subsection, we present the different shapes of the CDF and PDF shown in Figures 1 and 2 respectively. Figure 3 illustrate six distinct forms of the conditional intensity function: constant, decreasing, bathtub, unimodal, modified bathtub, and increasing intensity.

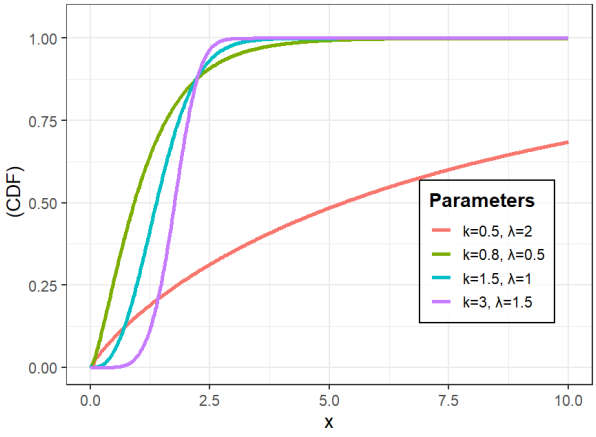

Figure 1. CDF of the Secant-Weibull distribution for different parameters

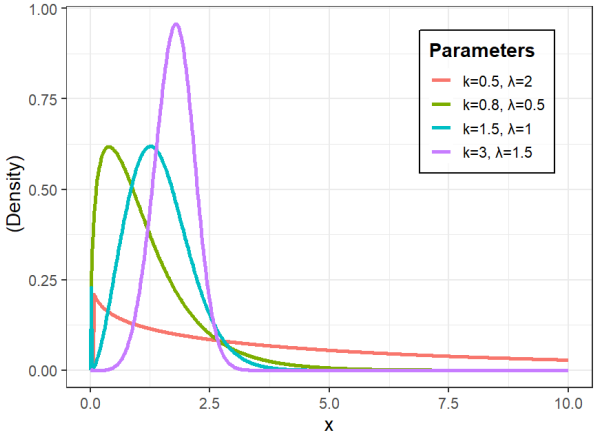

Figure 2. PDF of the Secant-Weibull distribution for different parameters

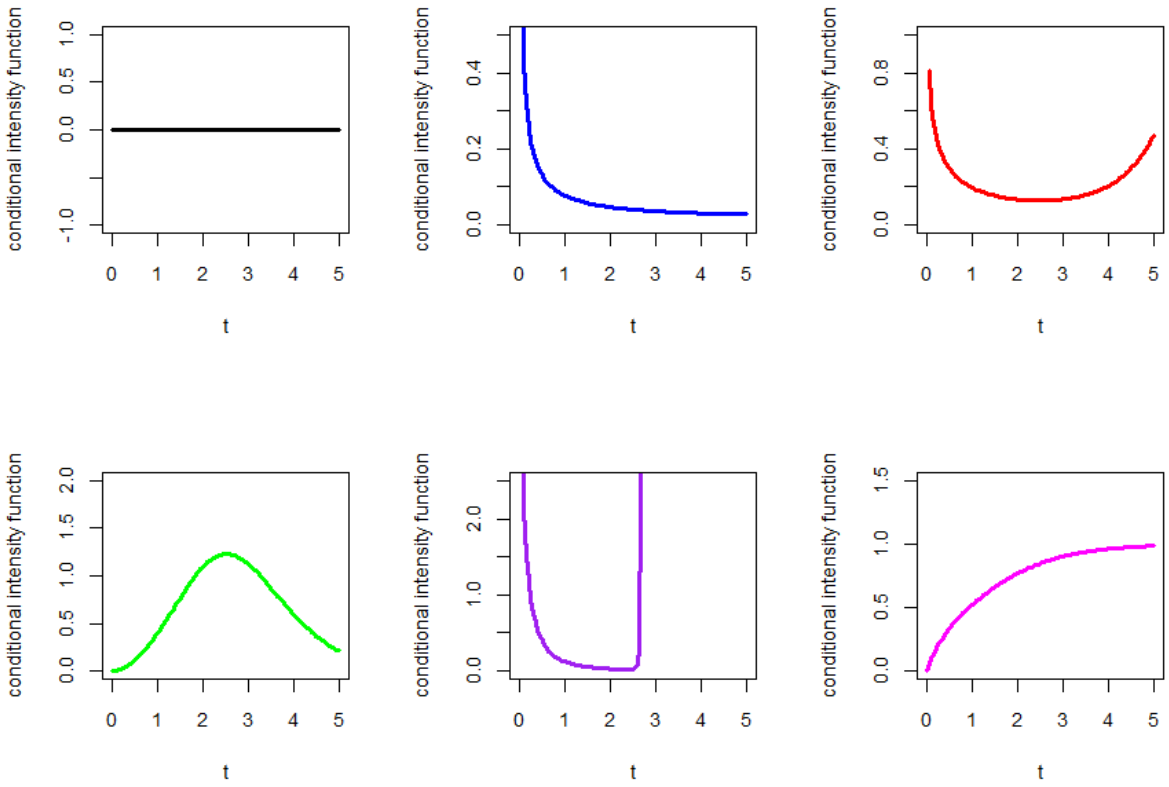

Figure 3. Conditional intensity shapes of the Secant-Weibull distribution

2.1.4. Further analytical characterizations for microstructure analysis

To evaluate the persistence, information flow, and risk dynamics of high-frequency durations, we derive three key properties of the SW distribution: Rényi Entropy, the expected Remaining Wait Time , and Order Statistics.

2.2. Rényi entropy

Rényi entropy measures the uncertainty or "disorder" in the timing of market events. It generalizes Shannon entropy and is particularly useful for understanding information flow in limit order books. For the

SW distribution, Rényi entropy of order v ($v > 0$, $v \neq 1$) for a random variable X with PDF $f(x)$ is defined as follows:

$$\mathrm{RE}_X(v) = \frac{1}{1-v} \log \left[\int_0^\infty f^v(x)\, dx \right]. \tag{6}$$

For the SW distribution with scale PDF is (4).
Substituting $f(x)$ into the integral gives

$$\int_0^\infty f^v(x)\, dx = \left(\frac{\pi k}{3\lambda}\right)^v \int_0^\infty \left(\frac{x}{\lambda}\right)^{v(k-1)} e^{-v(x/\lambda)^k} \left[\sec\left(\frac{\pi}{3}(1-e^{-(x/\lambda)^k})\right) \tan\left(\frac{\pi}{3}(1-e^{-(x/\lambda)^k})\right)\right]^v dx. \tag{7}$$

Expanding the trigonometric term via a series and applying the binomial theorem,we get

$$\left[\sec\left(\frac{\pi}{3}(1-e^{-(x/\lambda)^k})\right) \tan\left(\frac{\pi}{3}(1-e^{-(x/\lambda)^k})\right)\right]^v = \sum_{m=0}^{\infty}\sum_{j=0}^{\infty} a_m(v) \binom{2m+v}{j} (-1)^j \left(\frac{\pi}{3}\right)^{2m+v} e^{-j(x/\lambda)^k}, \tag{8}$$

where the coefficients $a_m(v)$ are determined from derivatives of $[\sec(s)\tan(s)]^v$ at $s = 0$.

Performing the change of variable $y = (x/\lambda)^k$ so that $x = \lambda y^{1/k}$ and $dx = \frac{\lambda}{k} y^{1/k-1} dy$, the integral becomes a gamma function:

$$\int_0^\infty \left(\frac{x}{\lambda}\right)^{v(k-1)} e^{-(v+j)(x/\lambda)^k} dx = \lambda k\, \Gamma\left(\frac{v(k-1)+1}{k}\right) (v+j)^{-(v(k-1)+1)/k}. \tag{9}$$

Substituting back, the Rényi entropy is

$$RE_X(v) = \frac{1}{1-v} \log \left[\Gamma\left(\frac{v(k-1)+1}{k}\right) \sum_{m=0}^{\infty}\sum_{j=0}^{\infty} a_m(v) \binom{2m+v}{j} (-1)^j \left(\frac{\pi}{3}\right)^{2m+v} \lambda k (v+j)^{-(v(k-1)+1)/k} \right]. \tag{10}$$

In financial contexts, higher entropy indicates a high degree of "market noise" or randomness in trade arrivals. Conversely, a decrease in entropy suggests a more structured arrival process, typically associated with periods of informed trading or institutional "meta-order" execution where durations become more predictable (clustering).

2.3. Expected remaining wait time

The expected Remaining Wait Time is crucial for algorithmic execution. It represents the expected time until the next trade occurs, given that t seconds have already elapsed since the last event. Within the framework of the SW distribution, this function is derived as:

$$m(t) = E[X - t \mid X > t] = \frac{1}{S(t)} \int_t^\infty S(x)\, dx.$$

For the Secant-Weibull specification with duration function $S(x) = 2 - \sec\left[\frac{\pi}{3}(1-e^{-(x/\lambda)^k})\right]$, this definition leads to the expression:

$$m(t) = \frac{\int_t^\infty \left\{2 - \sec\left[\frac{\pi}{3}\left(1-e^{-(x/\lambda)^k}\right)\right]\right\} dx}{2 - \sec\left[\frac{\pi}{3}\left(1-e^{-(t/\lambda)^k}\right)\right]}.$$

For a liquidity provider, $m(t)$ measures the "Expected Remaining Wait Time." Unlike the standard Weibull model, which imposes monotonic waiting times, the SW distribution allows for a bathtub-shaped trajectory . This captures a realistic market scenario where, if a long period passes without a trade, the expected time until the next trade may actually increase as the market becomes illiquid or "stale."

2.4. Order statistics

To quantify the behavior of the fastest trades (HFT activity) and the longest gaps (liquidity dry-ups), we utilize order statistics. Let $X_{(i)}$ denote the i-th order statistic in a sample of n durations. The probability density function (PDF) of $X_{(i)}$ is given by:

$$f_{i:n}(x) = \frac{n!}{(i-1)!(n-i)!} f(x)[F(x)]^{i-1}[1-F(x)]^{n-i}, \tag{11}$$

where $f(x)$ and $F(x)$ are the PDF and CDF of the underlying duration distribution. Substituting specific form $f(x)$ and $F(x)$ into Eq. (11) yields the distribution of extreme duration events.

$$\begin{aligned} f_{i:n}(x) =& \frac{n!}{(i-1)!(n-i)!} \cdot \left[\frac{\pi k}{3\lambda}\left(\frac{x}{\lambda}\right)^{k-1} e^{-(x/\lambda)^k}\right] \times \sec\left[\frac{\pi}{3}\left(1-e^{-(x/\lambda)^k}\right)\right] \tan\left[\frac{\pi}{3}\left(1-e^{-(x/\lambda)^k}\right)\right] \\ & \times \left[\sec\left[\frac{\pi}{3}\left(1-e^{-(x/\lambda)^k}\right)\right]-1\right]^{i-1} \times \left[2-\sec\left[\frac{\pi}{3}\left(1-e^{-(x/\lambda)^k}\right)\right]\right]^{n-i}. \end{aligned}$$

In the context of high-frequency trading, the extreme values of trade durations provide critical insights into market microstructure. The first order statistic $X_{(1)}$ represents the "Maximum Market Speed" in a sample, while the n-th statistic $X_{(n)}$ captures the "Maximum Liquidity Gap." This formulation is essential for stress-testing trading algorithms against "flash-clumps" (many trades in milliseconds) or "flash-crashes" (total cessation of trading).

The first Order Statistic :the minimum duration $X_{(1)}$ ($i = 1$), the PDF simplifies to

$$\begin{aligned} f_{X_{(1)}}(x) &= n\, f(x)\, [1-F(x)]^{n-1} \\ &= n \cdot \left[\frac{\pi k}{3\lambda}\left(\frac{x}{\lambda}\right)^{k-1} e^{-(x/\lambda)^k}\right] \times \sec\left[\frac{\pi}{3}\left(1-e^{-(x/\lambda)^k}\right)\right] \tan\left[\frac{\pi}{3}\left(1-e^{-(x/\lambda)^k}\right)\right] \\ &\quad \times \left[2-\sec\left[\frac{\pi}{3}\left(1-e^{-(x/\lambda)^k}\right)\right]\right]^{n-1}. \end{aligned}$$

The n-the Order Statistic :the maximum duration $X_{(n)}$ ($i = n$), the PDF simplifies to

$$\begin{aligned} f_{X_{(n)}}(x) &= n\, f(x)\, [F(x)]^{n-1} \\ &= n \cdot \left[\frac{\pi k}{3\lambda}\left(\frac{x}{\lambda}\right)^{k-1} e^{-(x/\lambda)^k}\right] \times \sec\left[\frac{\pi}{3}\left(1-e^{-(x/\lambda)^k}\right)\right] \tan\left[\frac{\pi}{3}\left(1-e^{-(x/\lambda)^k}\right)\right] \\ &\quad \times \left[\sec\left[\frac{\pi}{3}\left(1-e^{-(x/\lambda)^k}\right)\right]-1\right]^{n-1}. \end{aligned}$$

These expressions are mathematically valid only for x satisfying the domain condition of the secant function, that is $0 \le (\pi/3)\left(1-e^{-(x/\lambda)^k}\right) < (\pi/2)$.

Figure 4 illustrates these properties: the right plot (Expected Remaining Wait Time) displays the bathtub shape essential for realistic liquidity modeling, while the left plot (Order Statistics) shows the distribution of extremes, which is crucial for algorithmic trading risk analysis.

2.5. The Secant-Weibull ACD model with calendar effects (SW-ACD-X)

The SW-ACD-X model characterizes durations as $x_i = \psi_i \epsilon_i$, where ϵ_i is a stochastic innovation and ψ_i is the conditional mean. To account for deterministic intraday patterns simultaneously with stochastic clustering, we specify the conditional mean as Eq. (2). where $Z_{i-1,1}$ represents exogenous calendar variables (time-of-day dummies). The standard SW-ACD model is recovered as a special case of this formulation when $\gamma_l = 0$ for all l. To ensure model identifiability and maintain the interpretation of ψ_i as the actual conditional expected duration, we impose the unit-mean constraint $E[\epsilon_i] = 1$.

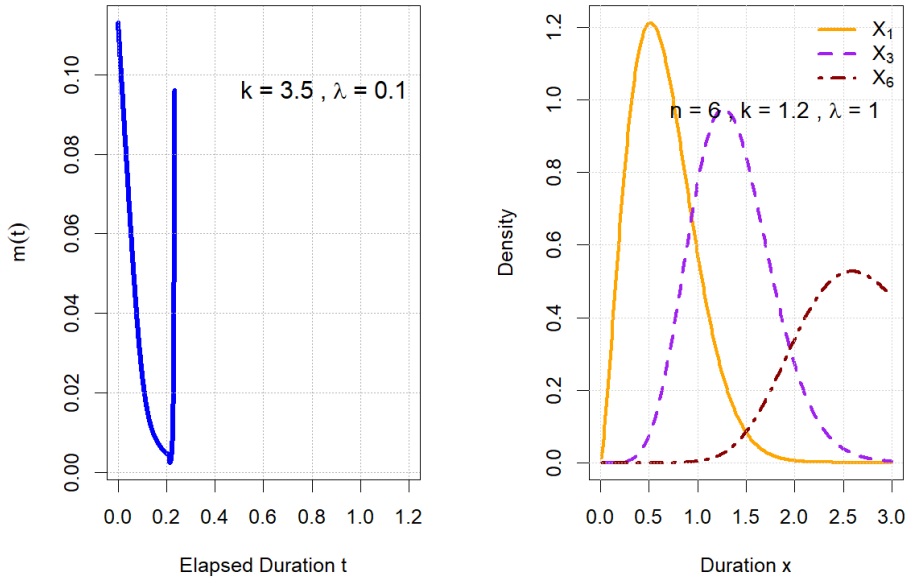

Figure 4. Right: MRL, Left: Order Statistics; of the Secant-Weibull distribution

2.5.1. Moment properties and identification constraint

The r-th raw moment of the SW distribution is essential for defining the structural properties of the innovation term. Substituting the PDF from Eq. (4) into the moment definition $\mathbb{E}[\epsilon^r] = \int_0^\infty x^r f(x)dx$, we obtain

$$\mu'_r = \mathbb{E}[\epsilon^r] = \frac{\pi k}{3\lambda} \int_0^\infty x^r \left(\frac{x}{\lambda}\right)^{k-1} e^{-(x/\lambda)^k} \sec\left[\frac{\pi}{3}\left(1 - e^{-(x/\lambda)^k}\right)\right] \tan\left[\frac{\pi}{3}\left(1 - e^{-(x/\lambda)^k}\right)\right] dx. \tag{12}$$

To evaluate this integral analytically, we utilize the power series expansion of the circular trigonometric product $\sec(z)\tan(z)$ via Euler numbers E_{2m+1}. The r-th moment is derived as

$$\mu'_r = \lambda^r \Gamma\left(1 + \frac{r}{k}\right) \sum_{m=0}^{\infty} \frac{E_{2m+1}}{(2m+1)!} \left(\frac{\pi}{3}\right)^{2m+2} \sum_{j=0}^{2m+1} \binom{2m+1}{j} \frac{(-1)^j}{(j+1)^{1+r/k}}, \tag{13}$$

where E_{2m+1} are the Euler numbers. To satisfy the ACD requirement $\mathbb{E}[\epsilon_i] = 1$, we set $r = 1$ and define the scaling factor Λ_k such that

$$\Lambda_k = \Gamma\left(1 + \frac{1}{k}\right) \sum_{m=0}^{\infty} \frac{E_{2m+1}}{(2m+1)!} \left(\frac{\pi}{3}\right)^{2m+2} \sum_{j=0}^{2m+1} \binom{2m+1}{j} \frac{(-1)^j}{(j+1)^{1+1/k}}. \tag{14}$$

By imposing the identification constraint $\lambda = 1/\Lambda_k$, the scale parameter becomes a restricted function of the shape parameter k. This reduces the parameter space by one dimension, preventing numerical redundancy and resolving the structural competition between the intercept ω and the scale parameter. This moment property and identification constraint are identical for both the SW–ACD and SW–ACD–X models. For numerical implementation, the infinite series in Eq. (14) is evaluated using a truncation at $M = 50$ terms, as follows:

$$\Lambda_k \approx \Gamma\left(1 + \frac{1}{k}\right) \sum_{m=0}^{50} \frac{E_{2m+1}}{(2m+1)!} \left(\frac{\pi}{3}\right)^{2m+2} \sum_{j=0}^{2m+1} \binom{2m+1}{j} \frac{(-1)^j}{(j+1)^{1+1/k}}. \tag{15}$$

The truncation error is rigorously controlled by the radius of convergence of the power series ($|z| < \pi/2$). Since the argument is $z = \pi/3$, the ratio $z/R = 2/3$ ensures a geometric decay of terms, allowing the approximation to reach machine precision ($< 10^{-16}$) at $M = 50$. Numerical stability is preserved for the

shape parameter range $0.5 < k < 5$ typically observed in financial durations, as the factorial growth in the denominator effectively offsets the growth of the Euler numbers.

2.5.2. Standardized innovation distribution

By substituting the identification constraint into the general density, the PDF of the standardized innovations $\epsilon_i \sim SW(k)$ is expressed as follows:

$$g(\epsilon_i;k) = \frac{\pi k \Lambda_k}{3}(\epsilon_i \Lambda_k)^{k-1} \exp\left[-(\epsilon_i \Lambda_k)^k\right] \cdot \sec\left[\frac{\pi}{3}\left(1 - e^{-(\epsilon_i \Lambda_k)^k}\right)\right] \tan\left[\frac{\pi}{3}\left(1 - e^{-(\epsilon_i \Lambda_k)^k}\right)\right], \quad \epsilon_i > 0. \tag{16}$$

This standardized innovation distribution is common to both the SW–ACD–X and the SW–ACD models.

2.5.3. Conditional PDF of duration

Given the transformation $\epsilon_i = x_i/\psi_i$ and the Jacobian $|d\epsilon_i/dx_i| = 1/\psi_i$, the conditional PDF of the observed duration x_i given the filtration $\mathcal{F}_{i-1}$ is

$$\begin{aligned} f(x_i \mid \mathcal{F}_{i-1};\boldsymbol{\theta}) &= \frac{1}{\psi_i} \cdot g\left(\frac{x_i}{\psi_i};k\right) \\ &= \frac{\pi k \Lambda_k}{3\psi_i}\left(\frac{x_i \Lambda_k}{\psi_i}\right)^{k-1} \exp\left[-\left(\frac{x_i \Lambda_k}{\psi_i}\right)^k\right] \times \sec\left[\frac{\pi}{3}\left(1 - \exp\left[-\left(\frac{x_i \Lambda_k}{\psi_i}\right)^k\right]\right)\right] \\ &\quad \times \tan\left[\frac{\pi}{3}\left(1 - \exp\left[-\left(\frac{x_i \Lambda_k}{\psi_i}\right)^k\right]\right)\right], \end{aligned} \tag{17}$$

where $\boldsymbol{\theta} = (\omega, \alpha_1, \beta_1, k)^\top$ is the parameter vector, and Λ_k is computed from k via Eq. (13).

2.5.4. Conditional quantile function

The SW–ACD–X model yields an analytical Quantile function that integrates the Autoregressive dynamics and the seasonal parameters γ_l. For a probability level $\tau \in (0,1)$, the τ-Quantile is given by:

$$Q_{x_i}(\tau|\mathcal{F}_{i-1}) = \frac{\psi_i}{\Lambda_k}\left[-\ln\left(1 - \frac{3}{\pi}\operatorname{arcsec}(\tau+1)\right)\right]^{1/k}. \tag{18}$$

where ψ_i is defined as in Eq. (2). this analytical formulation facilitates both Monte Carlo simulation and direct likelihood evaluation for parameter estimation, while nesting the SW–ACD model as a special case where $\gamma_l = 0$ for all l.

2.5.5. Conditional intensity function

The conditional intensity function $h(x_i \mid \mathcal{F}_{i-1})$ provides crucial insights into market dynamics by quantifying the instantaneous probability of a trade occurring given the time elapsed since the last transaction and past market information. The formula of conditional intensity function is:

$$h(x_i \mid \mathcal{F}_{i-1}) = \frac{\frac{\pi k \Lambda_k}{3\psi_i}(x_i \Lambda_k/\psi_i)^{k-1} \exp\left[-(x_i \Lambda_k/\psi_i)^k\right] \sec\left(\frac{\pi}{3}\left[1 - e^{-(x_i \Lambda_k/\psi_i)^k}\right]\right) \tan\left(\frac{\pi}{3}\left[1 - e^{-(x_i \Lambda_k/\psi_i)^k}\right]\right)}{2 - \sec\left(\frac{\pi}{3}\left[1 - e^{-(x_i \Lambda_k/\psi_i)^k}\right]\right)}. \tag{19}$$

The conditional intensity function $h(x_i \mid \mathcal{F}_{i-1})$ characterizes the instantaneous probability of an event, dynamically scaled by the conditional mean ψ_i to reflect varying market speeds. Its unique trigonometric specification allows the model to capture complex, non-monotonic conditional intensity such as consolidation periods and momentum building while the standardization Λ_k ensures that the innovation process remains scale-invariant with a unit mean.

2.6. Model estimation

This section details the estimation procedures for the Secant-Weibull distribution and the subsequent ACD frameworks, utilizing both Frequentist and Bayesian paradigms. Frequentist estimation is conducted via (MLE), while Bayesian inference is implemented using (HMC) with the (NUTS). The numerical properties of the SW distribution allow for flexible and complex shapes in the conditional intensity of durations across both frameworks.

2.6.1. Frequentist estimation of SW distribution

The parameter vector of the SW distribution, $\boldsymbol{\theta} = (\lambda, k)^\top$, is estimated using the (MLE) method. By maximizing the likelihood function associated with the observed data, the frequentist estimates of the parameters λ and k are obtained.

Let $\mathbf{x} = (x_1, x_2, \ldots, x_n)$ denote a random sample of n independent and identically distributed (i.i.d.) observations drawn from the SW distribution. The likelihood function $L(\boldsymbol{\theta} \mid \mathbf{x})$is defined as the joint probability density of the sample and is given by

$$L(\boldsymbol{\theta} \mid \mathbf{x}) = \prod_{i=1}^{n} \left[\frac{\pi}{3} \cdot \frac{k}{\lambda} \left(\frac{x_i}{\lambda} \right)^{k-1} e^{-(x_i/\lambda)^k} \cdot \sec\left(\frac{\pi}{3} \left(1 - e^{-(x_i/\lambda)^k} \right) \right) \cdot \tan\left(\frac{\pi}{3} \left(1 - e^{-(x_i/\lambda)^k} \right) \right) \right]. \tag{20}$$

The log-likelihood function is obtained by taking the natural logarithm of the likelihood function, as follows:

$$\ell(\boldsymbol{\theta} \mid \mathbf{x}) = \sum_{i=1}^{n} \ln \left[\frac{\pi}{3} \cdot \frac{k}{\lambda} \left(\frac{x_i}{\lambda} \right)^{k-1} e^{-(x_i/\lambda)^k} \cdot \sec\left(\frac{\pi}{3} \left(1 - e^{-(x_i/\lambda)^k} \right) \right) \cdot \tan\left(\frac{\pi}{3} \left(1 - e^{-(x_i/\lambda)^k} \right) \right) \right].$$

2.6.2. Estimation of the SW–ACD and SW–ACD–X Frameworks

When accounting for temporal dependencies and intraday seasonality, the observed durations x_i are no longer i.i.d. Instead, they are modeled as $x_i = \psi_i \epsilon_i$, where the stochastic innovations follow a Secant-Weibull distribution, denoted as $\epsilon_i \sim \mathrm{SW}(k)$. The parameter vector to be estimated is defined as $\boldsymbol{\theta} = (\omega, \alpha_1, \beta_1, \gamma_1, k)^\top$.

While the specification of the conditional mean ψ_i differs between the standard SW–ACD and the SW–ACD–X (the latter incorporating calendar effects γ_l), both models share the same conditional density structure. We estimate the parameters by maximizing the conditional log-likelihood. Given the information set $\mathcal{F}_{i-1}$, the density of x_i is determined by the innovation distribution, and the conditional likelihood function is

$$\begin{aligned} L(\boldsymbol{\theta} \mid \mathbf{x}) &= \prod_{i=1}^{n} f(x_i \mid \mathcal{F}_{i-1}; \boldsymbol{\theta}) \\ &= \prod_{i=1}^{n} \left[\frac{\pi k \Lambda_k}{3\psi_i} \left(\frac{x_i \Lambda_k}{\psi_i} \right)^{k-1} \exp\left[-\left(\frac{x_i \Lambda_k}{\psi_i} \right)^k \right] \times \sec\left[\frac{\pi}{3} \left(1 - \exp\left[-\left(\frac{x_i \Lambda_k}{\psi_i} \right)^k \right] \right) \right] \right. \\ &\quad \left. \times \tan\left[\frac{\pi}{3} \left(1 - \exp\left[-\left(\frac{x_i \Lambda_k}{\psi_i} \right)^k \right] \right) \right] \right]. \end{aligned}$$

Taking natural logarithms, the conditional log-likelihood function $\ell(\theta)$ is expressed as

$$\begin{aligned} \ell(\boldsymbol{\theta} \mid \mathbf{x}) = \sum_{i=1}^{n} \left(\ln\left(\frac{\pi}{3} \right) + \ln(k) + k \ln(\Lambda_k) - k \ln(\psi_i) + (k-1) \ln(x_i) - \left[\frac{x_i \Lambda_k}{\psi_i} \right]^k \right. \\ \left. + \ln\left[\sec\left(\frac{\pi}{3} \left(1 - \exp\left[-\left(\frac{x_i \Lambda_k}{\psi_i} \right)^k \right] \right) \right) \right] + \ln\left[\tan\left(\frac{\pi}{3} \left(1 - \exp\left[-\left(\frac{x_i \Lambda_k}{\psi_i} \right)^k \right] \right) \right) \right] \right). \end{aligned}$$

The SW–ACD model is nested within this framework and can be estimated by imposing the restriction $\gamma_l = 0$ for all l.

The maximum likelihood estimates $\hat{\boldsymbol{\theta}}$ cannot be obtained analytically due to the recursive form of the conditional mean ψ_i and the nonlinearity of the Secant–Weibull density. Therefore, the log-likelihood must be maximized using iterative numerical methods, such as the BFGS algorithm, to estimate the parameters. To initialize the recursion for ψ_i at $i = 1$, the pre-sample values (x_0, ψ_0) and the exogenous variables $Z_{l,0}$ are set equal to their respective sample means. During maximum likelihood estimation, these initial values are treated as fixed constants rather than parameters to be estimated.

2.6.3. Bayesian Secant-Weibull distribution

Parameters are regarded as random variables with prior distributions in the Bayesian method. The posterior distributions are obtained by updating these priors with the observed data using the Bayes theorem. Given the data $\mathbf{x} = (x_1, \ldots, x_n)$ for the Secant–Weibull distribution, the joint posterior distribution of the parameters λ and k is:

$$p(\lambda, k \mid x) \propto p(x \mid \lambda, k) \cdot p(\lambda) \cdot p(k).$$

2.6.4. Prior Specification

For the Secant-Weibull parameters, we specify conditionally independent priors:

$$k \sim \text{Gamma}(a_1, c_1), \quad p(k) = \frac{c_1^{a_1}}{\Gamma(a_1)} k^{a_1-1} e^{-c_1 k}, \quad k > 0, a_1 > 0, c_1 > 0,$$

$$\lambda \sim \text{Gamma}(a_2, c_2), \quad p(\lambda) = \frac{b_2^{a_2}}{\Gamma(a_2)} \lambda^{a_2-1} e^{-c_2 \lambda}, \quad \lambda > 0, a_2 > 0, c_2 > 0,$$

with hyperparameters $a_1, c_1, a_2, c_2 > 0$. The Gamma prior ensures positivity and provides flexibility in representing prior beliefs about the scale and shape parameters.

2.6.5. Posterior distribution

The joint posterior distribution combining the likelihood from Eq. (18) with the priors is:

$$\begin{aligned} p(\boldsymbol{\theta} \mid \mathbf{x}) &\propto \left[\prod_{i=1}^{n} f(x_i; \lambda, k) \right] \times p(\lambda) \times p(k) \\ &= \left[\prod_{i=1}^{n} \frac{\pi}{3} \cdot \frac{k}{\lambda} \left(\frac{x_i}{\lambda} \right)^{k-1} e^{-(x_i/\lambda)^k} \times \sec\left(\frac{\pi}{3} \left(1 - e^{-(x_i/\lambda)^k} \right) \right) \cdot \tan\left(\frac{\pi}{3} \left(1 - e^{-(x_i/\lambda)^k} \right) \right) \right] \\ &\quad \times \frac{c_2^{a_2}}{\Gamma(a_2)} \lambda^{a_2-1} e^{-c_2 \lambda} \times \frac{c_1^{a_1}}{\Gamma(a_1)} k^{a_1-1} e^{-c_1 k}. \end{aligned}$$

Using the NUTS sampler, we estimate the posterior distributions for k and λ with Gamma priors for both parameters. The model's performance is assessed through MCMC diagnostics, ensuring that the potential scale reduction factor ($\hat{R}$) is close to 1.00 and that the effective sample size is adequate for reliability .

2.6.6. Bayesian SW–ACD and SW–ACD–X Models

Bayesian inference provides a probabilistic framework for parameter estimation by combining prior information with observed data through Bayes' theorem [11]. In this framework, prior distributions represent initial beliefs about the parameters, which are updated using the likelihood of the observed durations to obtain the posterior distribution.

2.7. Model identification and parameter constraints

To avoid the structural identification redundancy between the scale of the ACD process (ω) and the scale parameter of the innovation distribution (λ), the scale parameter is not estimated directly. Instead, it is treated as a deterministic function of the shape parameter k such that $\lambda = 1/\Lambda_k$, where Λ_k is the normalizing constant that ensures the unit mean constraint $E[\epsilon_i] = 1$. Under this identified specification, the parameter vectors are

defined as $\boldsymbol{\theta} = (\omega, \alpha_1, \beta_1, k)^\top$ for the SW–ACD model, and $\boldsymbol{\theta}_X = (\omega, \alpha_1, \beta_1, \gamma_1, k)^\top$ for the SW–ACD–X model that incorporates calendar-effects.

2.8. Prior distributions

Weakly informative priors are assigned to ensure that the likelihood dominates the posterior inference while maintaining valid parameter domains, as follows:

$$\omega \sim \text{Gamma}(a_3, c_3), \quad p(\omega) = \frac{c_3^{a_3}}{\Gamma(a_3)} \omega^{a_3-1} e^{-c_3\omega}.$$

$$\alpha_1 \sim \text{Beta}(a_4, b_4), \quad p(\alpha_1) = \frac{\Gamma(a_4+b_4)}{\Gamma(a_4)\Gamma(b_4)} \alpha_1^{a_4-1}(1-\alpha_1)^{b_4-1}.$$

$$\beta_1 \sim \text{Beta}(a_5, b_5), \quad p(\beta_1) = \frac{\Gamma(a_5+b_5)}{\Gamma(a_5)\Gamma(b_5)} \beta_1^{a_5-1}(1-\beta_1)^{b_5-1}.$$

For the SW-ACD-X model, the calendar-effect coefficients follow Normal priors,as follows:

$$\gamma_l \sim \text{Normal}(a_6, c_6), \quad p(\gamma_l) = \frac{1}{\sqrt{2\pi c_6}} \exp\left[-\frac{(\gamma_l - a_6)^2}{2c_6}\right].$$

2.9. Posterior distribution

The posterior distribution, $p(\boldsymbol{\theta} \mid \mathbf{x})$, is derived by combining the conditional likelihood of the SW–ACD model with the joint prior distribution via Bayes' theorem,as follows:

$$p(\boldsymbol{\theta} \mid \mathbf{x}) \propto L(\mathbf{x} \mid \boldsymbol{\theta}) \cdot p(\boldsymbol{\theta}).$$

The joint prior $p(\boldsymbol{\theta})$ is the product of the individual marginal distributions:

$$p(\boldsymbol{\theta}) = p(\omega) \cdot p(\alpha_1) \cdot p(\beta_1) \cdot p(k). \tag{21}$$

For the SW-ACD(1,1) model, the joint posterior distribution is proportional to

$$\begin{aligned} p(\boldsymbol{\theta} \mid \mathbf{x}) \propto \prod_{i=1}^{n} \Bigg[& \frac{\pi k \Lambda_k}{3\psi_i} \left(\frac{x_i \Lambda_k}{\psi_i}\right)^{k-1} \exp\left[-\left(\frac{x_i\Lambda_k}{\psi_i}\right)^k\right] \times \sec\left(\frac{\pi}{3}\left[1-\exp\left[-\left(\frac{x_i\Lambda_k}{\psi_i}\right)^k\right]\right]\right) \\ & \times \tan\left(\frac{\pi}{3}\left[1-\exp\left[-\left(\frac{x_i\Lambda_k}{\psi_i}\right)^k\right]\right]\right)\Bigg] \times \frac{c_1^{a_1}}{\Gamma(a_1)} k^{a_1-1} e^{-c_1 k} \times \frac{c_3^{a_3}}{\Gamma(a_3)} \omega^{a_3-1} e^{-c_3\omega} \\ & \times \frac{\Gamma(a_4+b_4)}{\Gamma(a_4)\Gamma(b_4)} \alpha_1^{a_4-1}(1-\alpha_1)^{b_4-1} \times \frac{\Gamma(a_5+b_5)}{\Gamma(a_5)\Gamma(b_5)} \beta_1^{a_5-1}(1-\beta_1)^{b_5-1}. \end{aligned} \tag{22}$$

For the SW–ACD–X specification, the posterior additionally incorporates the priors of the calendar-effect parameters,as follows:

$$p(\boldsymbol{\theta}_X \mid \mathbf{x}) \propto L(\mathbf{x} \mid \boldsymbol{\theta}_X)\, p(\omega)\, p(\alpha_1)\, p(\beta_1)\, p(k) \prod_{l=1}^{m} p(\gamma_l),$$

$$\begin{aligned} p(\boldsymbol{\theta}_X \mid \mathbf{x}) \propto \prod_{i=1}^{n} \Bigg[& \frac{\pi k \Lambda_k}{3\psi_i} \left(\frac{x_i \Lambda_k}{\psi_i}\right)^{k-1} \exp\left[-\left(\frac{x_i\Lambda_k}{\psi_i}\right)^k\right] \times \sec\left(\frac{\pi}{3}\left[1-\exp\left[-\left(\frac{x_i\Lambda_k}{\psi_i}\right)^k\right]\right]\right) \\ & \times \tan\left(\frac{\pi}{3}\left[1-\exp\left[-\left(\frac{x_i\Lambda_k}{\psi_i}\right)^k\right]\right]\right)\Bigg] \times \frac{c_1^{a_1}}{\Gamma(a_1)} k^{a_1-1} e^{-c_1 k} \times \frac{c_3^{a_3}}{\Gamma(a_3)} \omega^{a_3-1} e^{-c_3\omega} \\ & \times \frac{\Gamma(a_4+b_4)}{\Gamma(a_4)\Gamma(b_4)} \alpha_1^{a_4-1}(1-\alpha_1)^{b_4-1} \times \frac{\Gamma(a_5+b_5)}{\Gamma(a_5)\Gamma(b_5)} \beta_1^{a_5-1}(1-\beta_1)^{b_5-1} \\ & \times \prod_{l=1}^{m} \left[\frac{1}{\sqrt{2\pi c_6}} \exp\left[-\frac{(\gamma_l - a_6)^2}{2c_6}\right]\right]. \end{aligned}$$

Because the posterior involves nonlinear trigonometric functions and recursive conditional means ψ_i, closed-form solutions are not available. Therefore, parameter estimation is performed using Markov Chain Monte Carlo (MCMC) methods. Specifically, this study employs Hamiltonian Monte Carlo (HMC) with the No-U-Turn Sampler (NUTS) implemented in Stan, which efficiently explores the high-dimensional posterior space and provides stable convergence [12].

2.10. Competing ACD–X Model specifications

To assess the empirical performance of the developed SW–ACD–X model, we compare it with four set up competing specifications. To confirm model identifiability, each innovation process has its unit mean ($E[\epsilon_i] = 1$) normalized. The following is a definition of the conditional log-likelihood functions for the competing specifications.

Weibull –ACD–X model. The conditional Log-Likelihood of W–ACD–X is given by

$$\ell(\theta) = \sum_{i=1}^{n} \left[\log\left(\frac{k}{\psi_i}\right) + \log\left(\left(\Gamma\left(1+\frac{1}{k}\right)\right)^k\right) + \log\left(\left(\frac{x_i}{\psi_i}\right)^{k-1}\right) - \left(\frac{x_i \cdot \Gamma\left(1+\frac{1}{k}\right)}{\psi_i}\right)^k \right]. \tag{23}$$

Gompertz–ACD–X Model. The conditional Log-Likelihood of G–ACD–X is given by

$$\ell(\theta) = n\ln(b) - \sum_{i=1}^{n} \ln(\psi_i) + b\sum_{i=1}^{n} x_i - \sum_{i=1}^{n} \left(\frac{e^{bx_i}-1}{\psi_i}\right). \tag{24}$$

Lomax–ACD–x model. The conditional log-likelihood of Lomax–ACD–X model is given by

$$\ell(\theta) = n\ln(k) - \sum_{i=1}^{n} \ln\left[\psi_i(k-1)\right] - (k+1)\sum_{i=1}^{n} \ln\left(1+\frac{x_i}{\psi_i(k-1)}\right). \tag{25}$$

log-weibull–ACD–X model. The conditional log-likelihood of LW–ACD–X model is given by

$$\ell(\theta) = \sum_{i=1}^{n} \left[\ln(k) + k\ln\left(\Gamma\left(1+\frac{1}{k}\right)\right) + (k-1)\ln(x_i) - k\ln(\psi_i) - \left(\Gamma\left(1+\frac{1}{k}\right)\frac{x_i}{\psi_i}\right)^k \right].$$

2.11. Model comparison

This section outlines the frequentist and Bayesian approaches employed to compare the proposed SW–ACD–X model with other competing specifications. These metrics allow us to determine the optimal model for capturing the complex dynamics of the data.

2.11.1. Frequentist model comparison

In the frequentist framework, model comparison balances goodness-of-fit with model complexity. This study employs two widely used information criteria: the Akaike Information Criterion (AIC), defined as $\text{AIC} = -2\ell(\hat{\boldsymbol{\theta}}) + 2p$, and the Bayesian Information Criterion (BIC), defined as $\text{BIC} = -2\ell(\hat{\boldsymbol{\theta}}) + p\ln(n)$, where $\ell(\hat{\boldsymbol{\theta}})$ denotes the maximized log-likelihood, p is the number of estimated parameters, and n is the sample size.

2.11.2. Bayesian model comparison

Bayesian model comparison focuses on predictive performance and model evidence, relying on the full posterior distribution rather than point estimates. In this study, model evaluation is conducted using the Watanabe–Akaike Information Criterion (WAIC) and Leave-One-Out Cross-Validation (LOOIC), both of which assess out-of-sample predictive accuracy based on posterior inference.

2.12. Simulation study

This section assesses the numerical stability, parameter identifiability, and finite-sample performance of the SW distribution and its dynamic expansions, namely the SW–ACD and SW–ACD–X models. We evaluate

the robustness of the suggested estimators in both static and dynamic data-generating environments using both Frequentist and Bayesian frameworks.

2.12.1. Design and data-generating process

Monte Carlo simulations are captured for sample sizes $n \in \{100, 200, \ldots, 1000\}$, with $R = 100$ independent replications for each design. The finite-sample performance of the estimators is assessed using the Average Bias (AB) and the Mean Squared Error (MSE), defined as

$$AB(\theta) = \frac{1}{N}\sum_{i=1}^{N}\left(\hat{\theta}^{(i)} - \theta\right), \tag{26}$$

$$MSE(\theta) = \frac{1}{N}\sum_{i=1}^{N}\left(\hat{\theta}^{(i)} - \theta\right)^2. \tag{27}$$

Recursively, durations are produced used inverse transform method and i.i.d.ϵ_i is first extracted from a unit-mean SW distribution . The Quantile function is then applied to uniform random variables $u \in (0, 1)$. Next, the observed durations are formed as $x_i = \psi_i \epsilon_i$, where ψ_i is the conditional mean. This process is equivalent to taking a direct sample at each time point i from the conditional Quantile function of the model.

2.12.2. Estimation methods

we use two different statistical methods. To have a thorough understanding of model dependability and parameter uncertainty.

2.12.3. Simulation design

The simulation is structured to assess three levels of model complexity:

1. *Baseline SW Distribution.* The parameter vector is $\boldsymbol{\theta} = (\lambda, k)$. We evaluate the MLE across sample sizes $n \in \{100, \ldots, 1000\}$ with $R = 100$ independent Monte Carlo replications. The true values are set at $\lambda = 0.8$ and $k = 1.2$.
2. *SW–ACD Model.* The dynamic parameter vector is $\boldsymbol{\theta} = (\omega, \alpha_1, \beta_1, k)$. True values are fixed at $\omega = 0.2, \alpha_1 = 0.15, \beta_1 = 0.7$, and $k = 1.2$. This setup assesses the model's ability to capture Autoregressive clustering.
3. *SW–ACD–X Model.* The vector expands to $\boldsymbol{\theta} = (\omega, \alpha_1, \beta_1, \gamma_1, k)$, where $\gamma_1 = 0.02$ represents a deterministic calendar effect. This design tests the simultaneous estimation of stochastic and exogenous components.

In the Bayesian framework, posterior recovery is assessed using a synthetic dataset of size $n = 1000$. Inference is conducted via the HMC–NUTS sampler in `Stan` using four parallel chains and 2,000 iterations (including 1,000 warm up draws). To ensure reproducibility, hyperparameters are set to weakly informative values: the intercept follows $\omega \sim \text{Gamma}(1, 10)$,while the scale and shape parameters follow $\lambda \sim \text{Gamma}(2, 2)$ and $k \sim \text{Gamma}(2, 2)$, respectively. For the Autoregressive parameters, we specify jointly truncated Beta priors over the stationarity simplex to strictly satisfy $\alpha_1 + \beta_1 < 1$, with $\alpha_1 \sim \text{Beta}(1.5, 15)$ and $\beta_1 \sim \text{Beta}(15, 1.5)$. The calendar effect coefficient is assigned a $\gamma_1 \sim \text{Normal}(0, 0.25)$ prior.

This setup ensures that the likelihood dominates the posterior while keeping parameters within their theoretically valid domains. Convergence is monitored via trace plots and the Gelman-Rubin diagnostic, ensuring all parameters achieve $\hat{R} < 1.01$.

2.13. Simulation results

2.13.1. Frequentist simulation results

The frequentist simulation results for the SW, SW–ACD, and SW–ACD–X models are summarized in Tables 1, 2, and 3, and visualized in Figures 5, 6, 7, and 8. The results indicate that while the MLEs are asymptotically consistent, they are not uniformly robust across all sample sizes. In the small-sample regime ($n = 100$), the dynamic SW–ACD and SW–ACD–X models exhibit sizable biases, particularly for the intercept

ω (positive bias ≈ 0.25) and the persistence parameter β_1 (negative bias ≈ -0.26). These outcomes reflect an identification challenge in sparse data environments, where the estimator struggles to disentangle baseline durations from Autoregressive clustering. Conversely, in the larger sample regime ($n \geq 700$), both bias and MSE diminish significantly, with absolute values approaching zero by $n = 1000$. Consequently, the proposed estimators are dependable for asymptotic inference and confidence interval generation, provided the sample size is sufficiently large to mitigate these inherent small-sample biases.

Table 1. Monte Carlo results for the SW distribution parameters

	λ		k	
n	Bias	MSE	Bias	MSE
100	0.0064	0.0051	0.0316	0.0286
200	-0.0014	0.0025	0.0134	0.0124
300	0.0008	0.0018	0.0043	0.0083
400	0.0000	0.0011	0.0048	0.0062
500	-0.0005	0.0009	0.0031	0.0045
600	0.0009	0.0008	0.0032	0.0042
700	-0.0010	0.0008	0.0008	0.0037
800	-0.0006	0.0006	0.0018	0.0032
900	-0.0006	0.0006	0.0009	0.0025
1000	0.0007	0.0005	0.0026	0.0024

Table 2. Monte Carlo simulation results for the SW–ACD model parameters

	ω		α_1		β_1		k	
n	Bias	MSE	Bias	MSE	Bias	MSE	Bias	MSE
100	0.2247	0.1393	0.0088	0.0083	-0.2449	0.1680	0.0198	0.0040
300	0.1203	0.0761	0.0032	0.0028	-0.1255	0.0878	0.0058	0.0012
500	0.0512	0.0313	-0.0010	0.0020	-0.0545	0.0390	0.0072	0.0008
700	0.0398	0.0147	0.0012	0.0013	-0.0409	0.0190	0.0029	0.0006
900	0.0168	0.0094	-0.0010	0.0010	-0.0180	0.0134	0.0056	0.0004

Table 3. Monte Carlo simulation results for the SW–ACD–X model parameters

	ω		α_1		β_1		γ_1		k	
n	Bias	MSE	Bias	MSE	Bias	MSE	Bias	MSE	Bias	MSE
100	0.2533	0.1628	0.0090	0.0085	-0.2650	0.1813	0.0109	0.0682	0.0250	0.0043
300	0.1167	0.0773	0.0036	0.0029	-0.1124	0.0811	-0.0216	0.0208	0.0073	0.0013
500	0.0447	0.0295	-0.0008	0.0021	-0.0484	0.0357	0.0101	0.0140	0.0081	0.0009
700	0.0522	0.0249	0.0022	0.0013	-0.0525	0.0283	0.0037	0.0090	0.0035	0.0006
900	0.0202	0.0106	-0.0007	0.0010	-0.0172	0.0133	-0.0189	0.0083	0.0062	0.0005

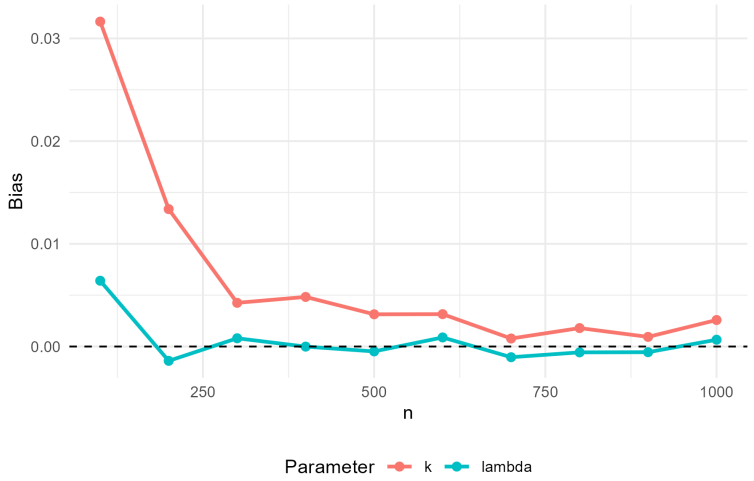

Figure 5. Plot of Bias for the SW distribution

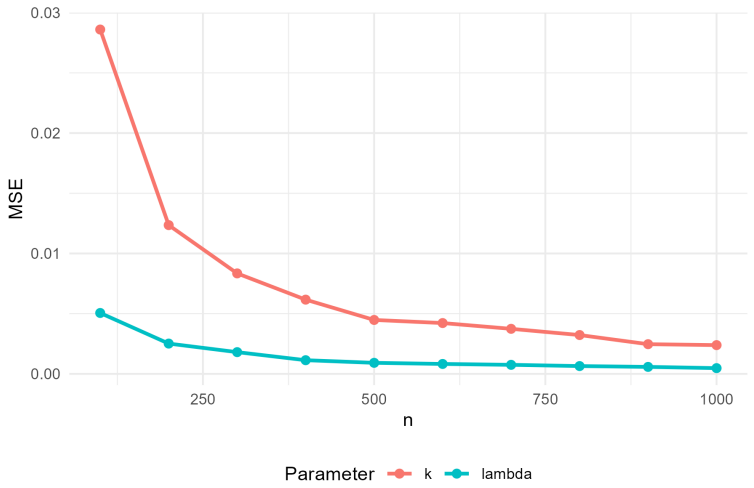

Figure 6. Plot of MSE for the SW distribution

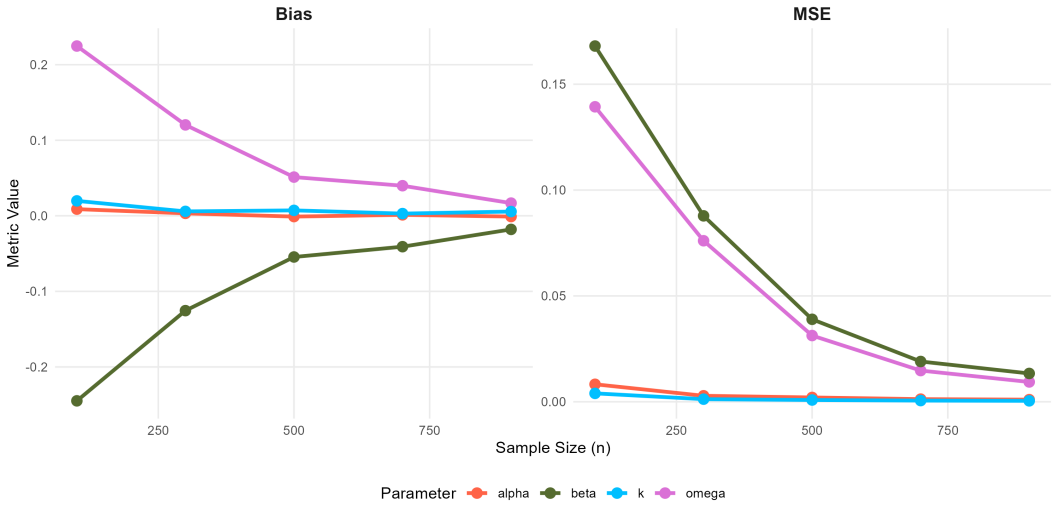

Figure 7. Bias and MSE for the SW-ACD model

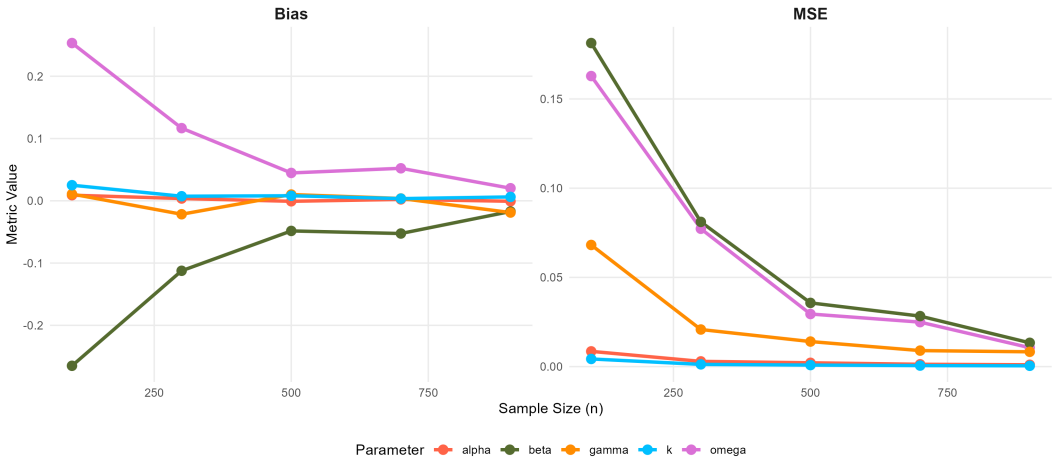

Figure 8. Bias and MSE for the SW-ACD-X model

2.13.2. Bayesian simulation results

The Bayesian estimation results for the SW, SW–ACD, and SW–ACD–X models Table 4 demonstrates a highly reliable and robust framework. MCMC diagnostics confirm numerical stability and convergence across all specifications. Specifically, the trace plots Figures 9 to 11 show well-mixed chains, and the autocorrelation plots Figures 12 to 14 exhibit rapid decay, ensuring that the posterior samples are independent. This stability is further supported by $\hat{R}$ values near 1.00 and high effective sample sizes ($n_{\text{eff}} > 1000$). Furthermore, parameter recovery is highly accurate; posterior means closely match the true values and fall within the 95% credible intervals. Notably, the successful identification of the calendar effect (γ_1) in the SW-ACD-X model proves that the framework is computationally efficient and statistically sound for application to real-world high-frequency financial data.

Table 4. Posterior summaries for the SW-distribution, SW–ACD model, and SW–ACD–X model

Model	Parameter	Mean	SD	2.5%	50%	97.5%	n_{eff}	Rhat
SW	λ	0.5119	0.0130	0.4843	0.5122	0.5372	1132	1.0044
	k	1.2167	0.0302	1.1554	1.2167	1.2751	1173	1.0043
SW–ACD	ω	0.0799	0.0264	0.0360	0.0773	0.1383	1415	1.0011
	α_1	0.0797	0.0129	0.0566	0.0789	0.1069	1059	1.0028
	β_1	0.8212	0.0307	0.7560	0.8229	0.8762	1019	1.0027
	k	1.2205	0.0302	1.1608	1.2196	1.2808	2092	1.0020
SW–ACD–X	ω	0.0966	0.0268	0.0514	0.0944	0.1561	1753	1.0001
	α_1	0.1141	0.0141	0.0873	0.1136	0.1449	1478	1.0012
	β_1	0.7479	0.0326	0.6791	0.7498	0.8076	1280	1.0010
	γ_1	0.0634	0.0192	0.0256	0.0635	0.0999	3169	1.0016
	k	1.1718	0.0290	1.1170	1.1712	1.2296	3114	1.0000

Figure 9. Trace plots for the SW-distribution parameters

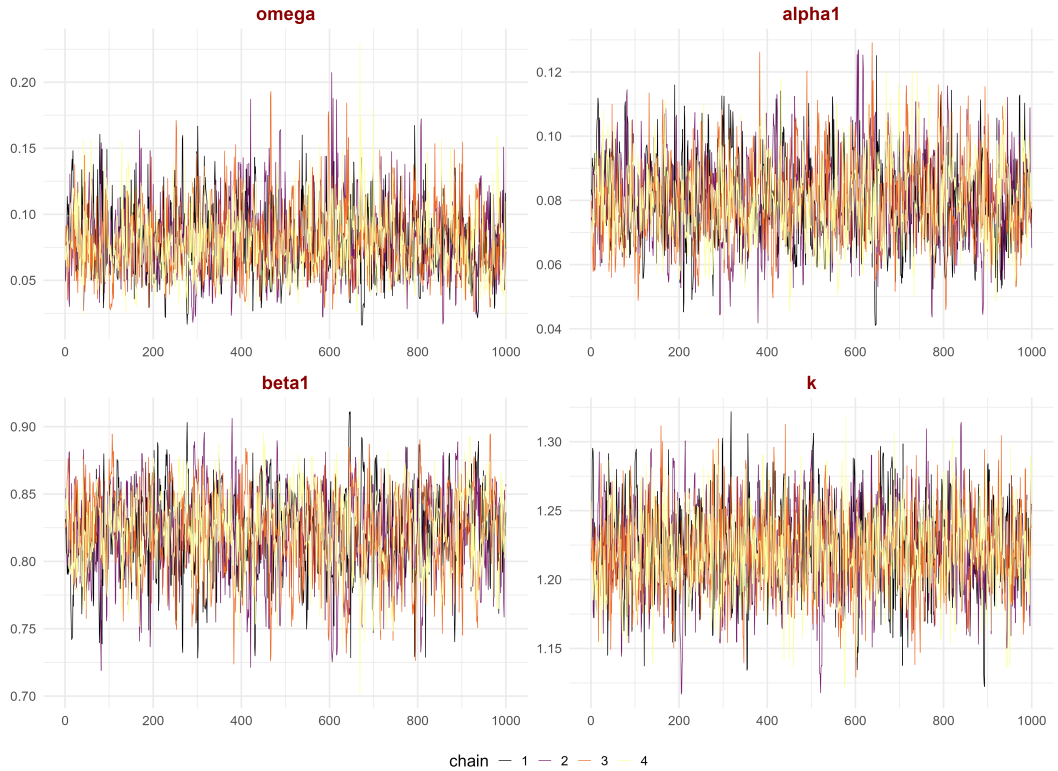

Figure 10. Trace plots for the SW–ACD model

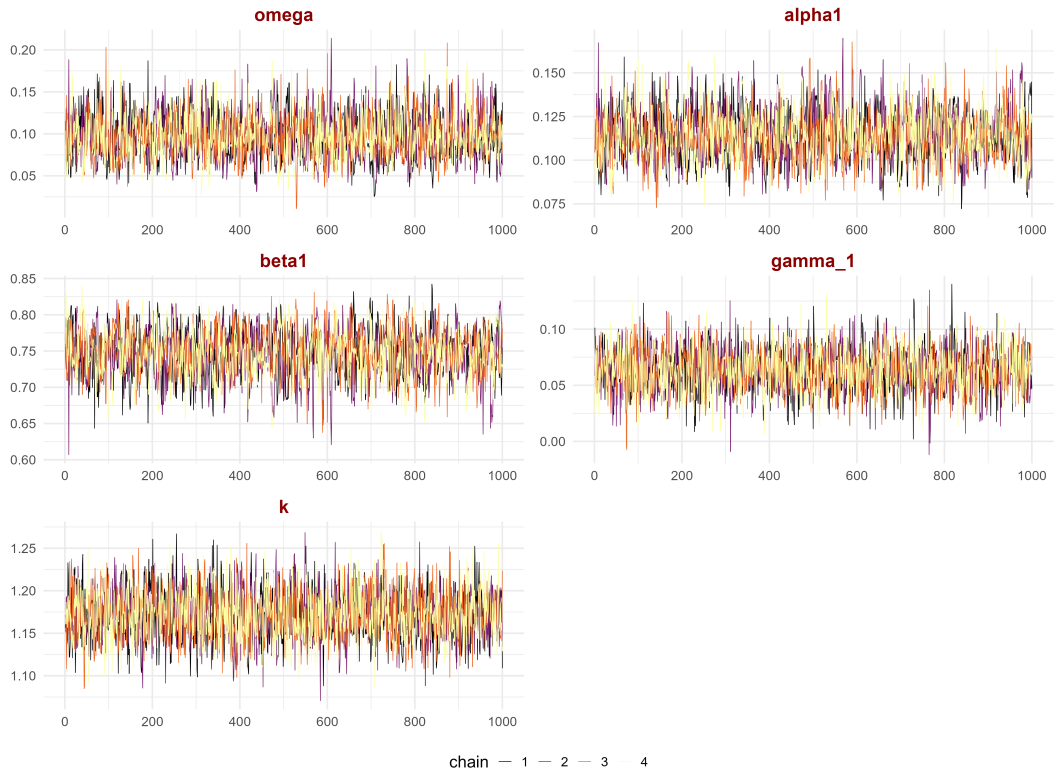

Figure 11. Trace plots for the SW–ACD–X model

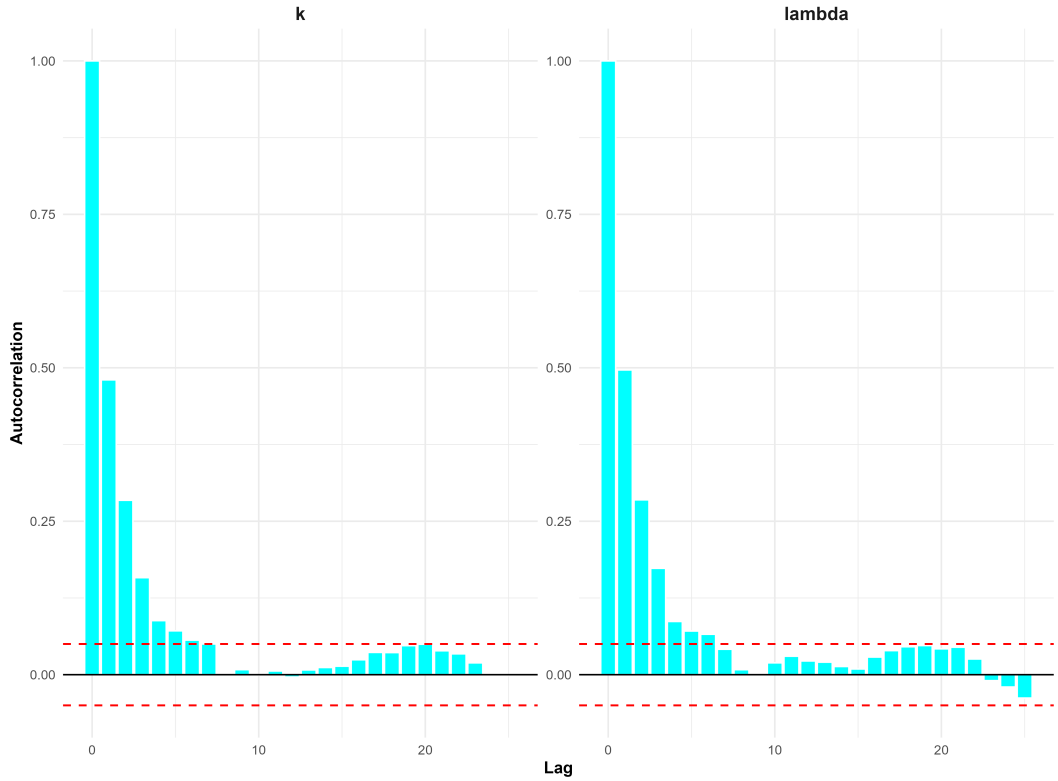

Figure 12. Autocorrelation plots of the SW-distribution

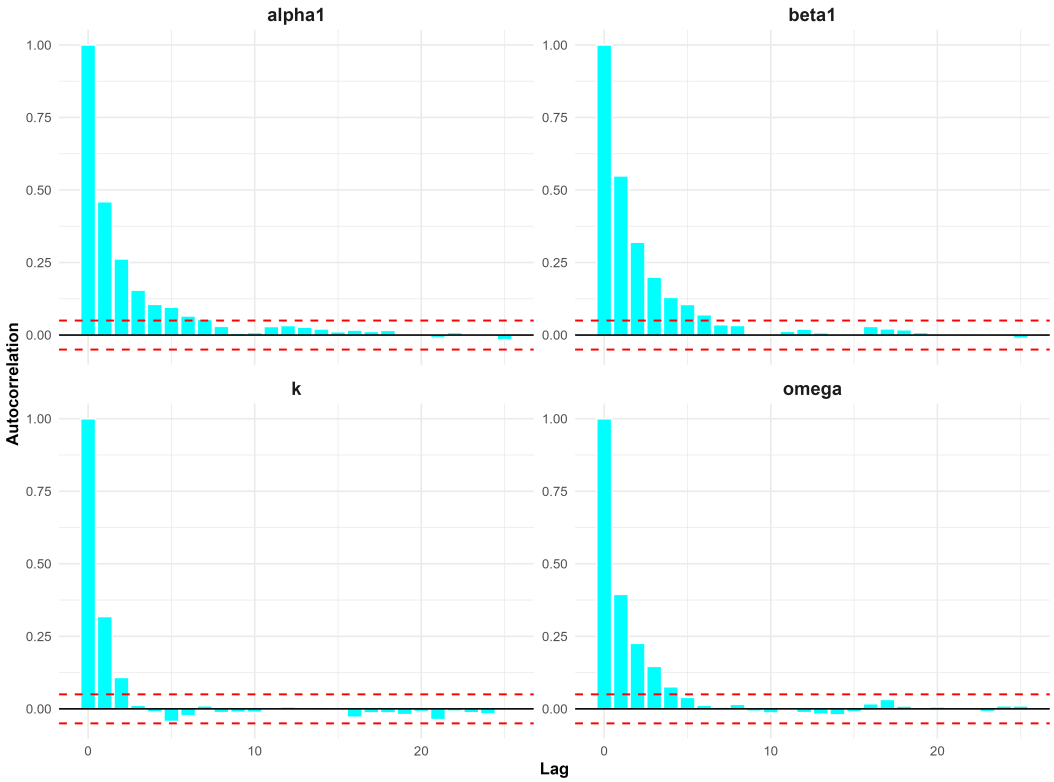

Figure 13. Autocorrelation plots of the SW–ACD model

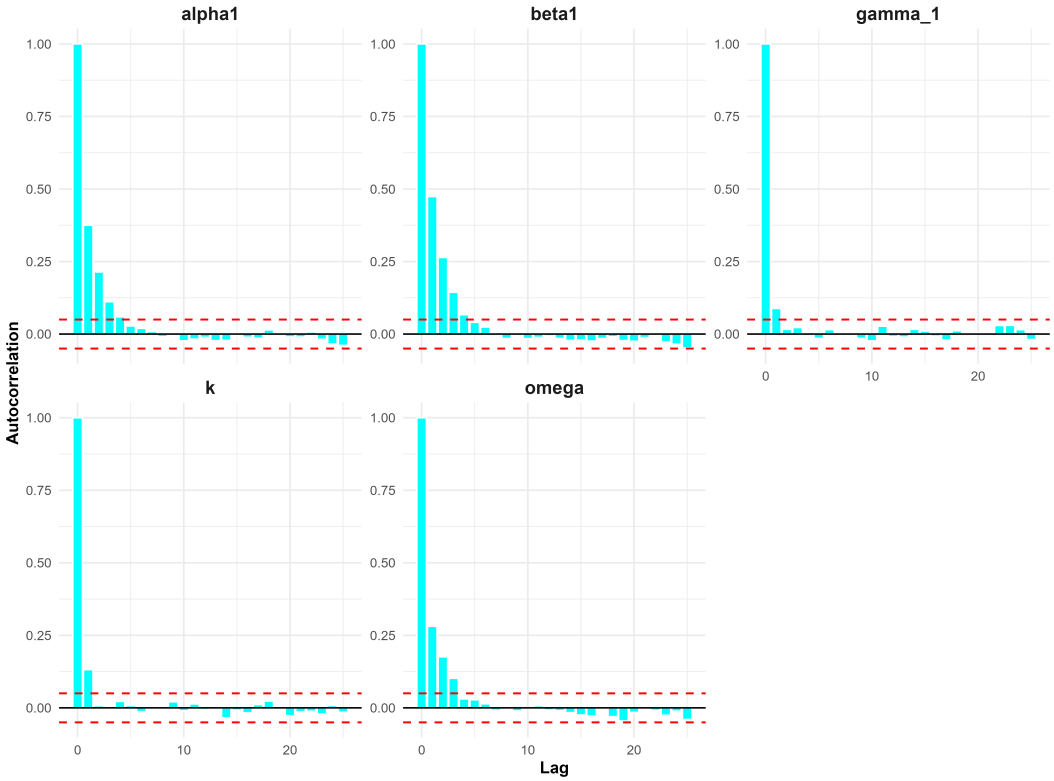

Figure 14. Autocorrelation plots of SW–ACD–X model

2.13.3. Model validation and estimation consistency

Posterior predictive checks confirm the structural adequacy of the Secant-Weibull specifications, with generated densities closely matching observed data. High estimation consistency is evidenced by the near-perfect alignment between frequentist MLEs (red dashed lines) and Bayesian posterior means (blue solid lines).

As shown in Figure 15, the model successfully recovers the shape parameter k while validating the trigonometric density. Figure 16 demonstrates similar precision for the persistence parameter β_1, where the MLE coincides with the posterior peak. Finally, Figure 17 confirms that the SW-ACD-X model accurately identifies the exogenous calendar effect γ_1. This convergence across all parameters (k, β_1, γ_1) highlights the numerical stability and superior generative performance of the proposed framework.

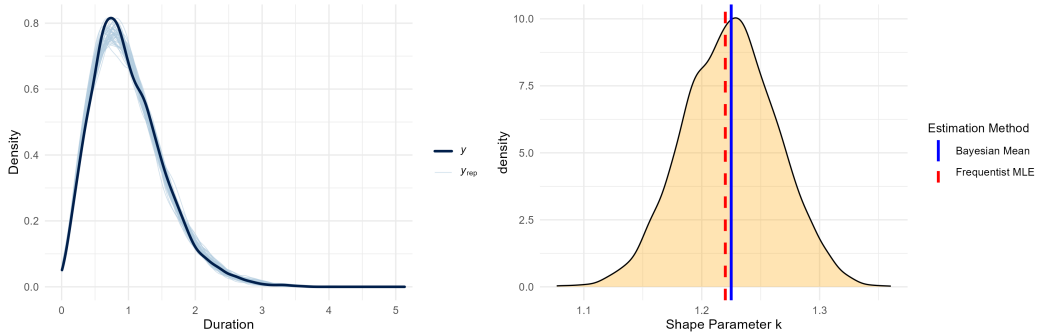

Figure 15. SW validation

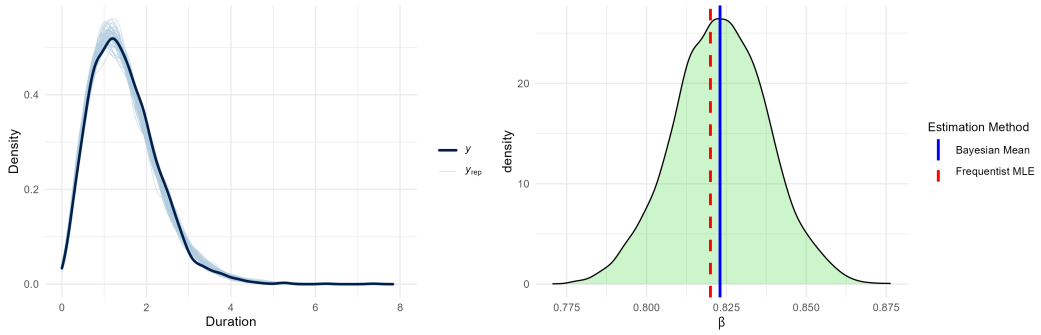

Figure 16. SW–ACD validation

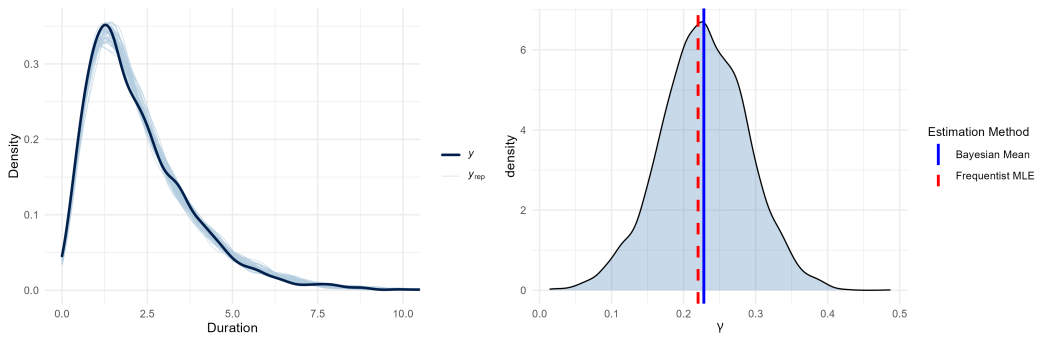

Figure 17. SW-ACD-X validation

3. Results

This section presents the empirical application of the SW-ACD-X model to high-frequency IBM transaction data. We conduct a comparative analysis against benchmarks like W–ACD–X, LW–ACD–X, Lomax–ACD–X, and G–ACD–X models, validating our specification through Frequentist and Bayesian frameworks. We assess model performance using the AIC and BIC for maximum likelihood, along with the WAIC and LOOIC for posterior analysis. This dual-method approach rigorously tests the SW–ACD–X model's efficiency in capturing heavy-tailed innovations and intraday calendar effects

3.1. Empirical data analysis

The empirical study utilizes 3,534 IBM transaction durations (x_i) sampled from the `ibm.txt` dataset covering November 1–7, 1990. After removing overnight gaps to isolate active trading sessions. Table 5 shows that the series displays high variability and positive skewness, meaning that most durations are short but occasionally very long. The density plot in Figure 18 supports this finding, revealing a clearly right-skewed and leptokurtic distribution. These features indicate heavy-tailed behavior, where extreme durations occur more often than under normality.

In terms of temporal dependence, the autocorrelation function in Figure 19 shows significant persistence across several lags, reflecting strong duration clustering and long-memory effects. Additionally, Figure 20 highlights clear intraday seasonality, with trading activity following a U-shaped pattern high at the market open and close and lower during midday.

Table 5. Statistical summary

Statistic	Mean	Median	Std. Dev	Minimum	Maximum	Skewness	Kurtosis
Duration	32.913	19	41.788	1	466	2.99	14.00

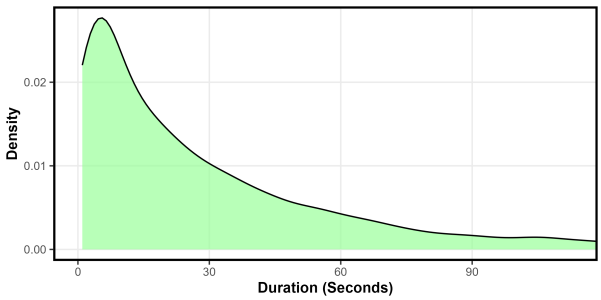

Figure 18. Density plot

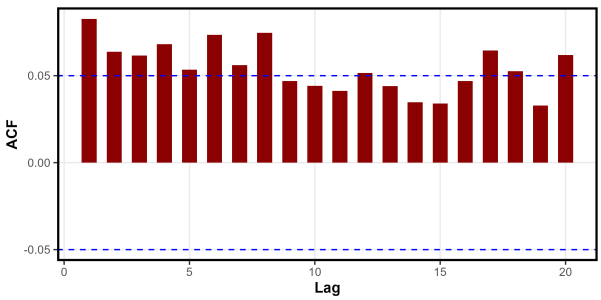

Figure 19. ACF plot

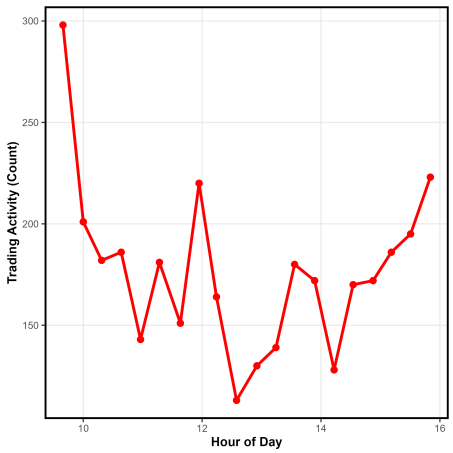

Figure 20. Intraday seasonality

3.1.1. Frequentist results

Table 6 demonstrates that the parameters are statistically significant for all five ACD–X frameworks, and the total of α_1 and β_1 are constantly approaching unity to suggest great duration persistence. Additionally, a persistent calendar effect is shown by the large negative estimates for γ_1, underscoring the significance of exogenous intraday seasonality in understanding duration dynamics.

Table 6. MLE estimates and standard errors

Model	Parameter	Estimate	Standard Error
SW–ACD–X	ω	0.039945	0.00582501
	α_1	0.061808	0.00638065
	β_1	0.899111	0.00003311
	γ_1	−0.006380	0.00218803
	k	0.562063	0.00728921
Lomax–ACD–X	ω	0.038920	0.00584951
	α_1	0.062239	0.00644485
	β_1	0.900361	0.00003315
	γ_1	−0.006119	0.00219196
	k	4.634004	0.48441160
W–ACD–X	ω	0.041658	0.00572901
	α_1	0.062016	0.00627033
	β_1	0.896670	0.00003302
	γ_1	−0.007084	0.00216018
	k	0.877165	0.01126426
LW–ACD–X	ω	0.040860	0.0062359
	α_1	0.062842	0.0088468
	β_1	0.878802	0.0209124
	γ_1	−0.010831	0.0034417
	k	0.880423	0.0112986
G–ACD–X	ω	0.007753	0.00205410
	α_1	0.010645	0.00171512
	β_1	0.842204	0.02467935
	γ_1	−0.001715	0.00052593
	k	0.100000	0.00915312

3.1.2. Frequentist model selection

Table 7 summarizes the SW–ACD–X model's performance in comparison to rival specifications. With the highest log-likelihood and the lowest information criteria values, the SW–ACD–X model exhibits superior fit and simplicity based on the Log-Likelihood, AIC, and BIC. Additionally, strong p-values from the

Ljung-Box diagnostic tests show that the model effectively takes duration clustering into account and leaves the standardized residuals free of significant autocorrelation.

Table 7. Model selection and diagnostic performance summary

Model	LogLik	AIC	BIC	LB_Stat	LB_pVal
SW–ACD–X	−3337.39	6684.78	6715.63	5.12	0.883
Lomax–ACD–X	−3347.85	6705.71	6736.56	5.15	0.881
W–ACD–X	−3362.83	6735.65	6766.50	5.16	0.880
LW–ACD–X	−3362.83	6735.65	6766.50	5.16	0.880
G–ACD–X	−3561.47	7132.94	7163.79	9.37	0.497

3.1.3. Bayesian results

This section summarizes the posterior distributions and convergence diagnostics for the proposed SW–ACD–X model and its benchmarks, confirming the stability and efficiency of the Bayesian estimation process across all specifications.

3.1.4. Numerical model diagnostics

Table 8 reports the posterior estimates of the ACD–X models under different distributional assumptions. Across all specifications, the persistence parameters indicate strong duration dependence, with $\alpha_1 + \beta_1$ remaining close to unity. The posterior means are well identified with reasonably tight credible intervals for most parameters. The covariate effect γ_1 is positive across all models, indicating a consistent influence of exogenous information on conditional durations. Convergence diagnostics are satisfactory for all models, as reflected by large effective sample sizes (*neff*) and $\hat{R}$ values close to one.

Table 8. Posterior estimates of ACD-X model parameters

Model	Param.	Mean	SD	2.5%	50%	97.5%	n_{eff}	$\hat{R}$
SW–ACD–X	ω	0.0220	0.0065	0.0114	0.0212	0.0371	1328	1.0035
	α_1	0.0289	0.0045	0.0205	0.0287	0.0386	1396	1.0023
	β_1	0.8783	0.0220	0.8286	0.8803	0.9149	1142	1.0043
	γ_1	-0.0036	0.0015	-0.0069	-0.0034	-0.0012	1844	1.0021
	k	0.5611	0.0074	0.5464	0.5611	0.5756	1852	1.0003
W–ACD–X	ω	0.0466	0.0137	0.0247	0.0445	0.0782	1575	1.0003
	α_1	0.0645	0.0101	0.0463	0.0638	0.0859	1681	1.0011
	β_1	0.8895	0.0198	0.8456	0.8918	0.9218	1390	1.0009
	γ_1	-0.0079	0.0032	-0.0150	-0.0076	-0.0027	1986	0.9993
	k	0.8766	0.0112	0.8544	0.8766	0.8981	2112	1.0017
LW–ACD–X	ω	0.0416	0.0133	0.0200	0.0400	0.0719	1166	1.0026
	α_1	0.0666	0.0115	0.0461	0.0658	0.0907	1357	1.0022
	β_1	0.9072	0.0175	0.8688	0.9088	0.9372	1022	1.0035
	γ_1	-0.0043	0.0028	-0.0107	-0.0040	0.0007	1684	1.0027
	k	1.3016	0.0151	1.2720	1.3016	1.3319	1891	1.0015
G–ACD–X	ω	0.0480	0.0119	0.0273	0.0469	0.0741	1183	1.0023
	α_1	0.0653	0.0091	0.0491	0.0646	0.0844	1286	1.0015
	β_1	0.8890	0.0171	0.8523	0.8903	0.9184	976	1.0031
	γ_1	-0.0084	0.0028	-0.0145	-0.0081	-0.0035	1662	1.0011
	b	0.0112	0.0011	0.0100	0.0109	0.0142	2537	1.0013
Lomax–ACD–X	ω	0.0446	0.0133	0.0231	0.0431	0.0749	1523	1.0010
	α_1	0.0653	0.0105	0.0462	0.0649	0.0866	1623	1.0017
	β_1	0.8921	0.0194	0.8497	0.8939	0.9258	1369	1.0017
	γ_1	-0.0070	0.0031	-0.0141	-0.0067	-0.0019	1954	0.9996
	k	4.6553	0.4796	3.8342	4.6212	5.6779	2053	1.0007

3.1.5. Visual diagnostics of MCMC convergence

Figure 21 shows the trace plots of the parameters for the proposed SW–ACD–X model. The chains move smoothly around constant levels and mix well across all iterations, which indicates that the MCMC algorithm has successfully converged to the target posterior distribution.

Figure 22 presents the corresponding autocorrelation function (ACF) plots. These plots show that autocorrelation decreases quickly and approaches zero after only a few lags. Together, the stable trace plots and low autocorrelation confirm the efficiency of the NUTS sampler and support the reliability of the Bayesian parameter estimates for the proposed model.

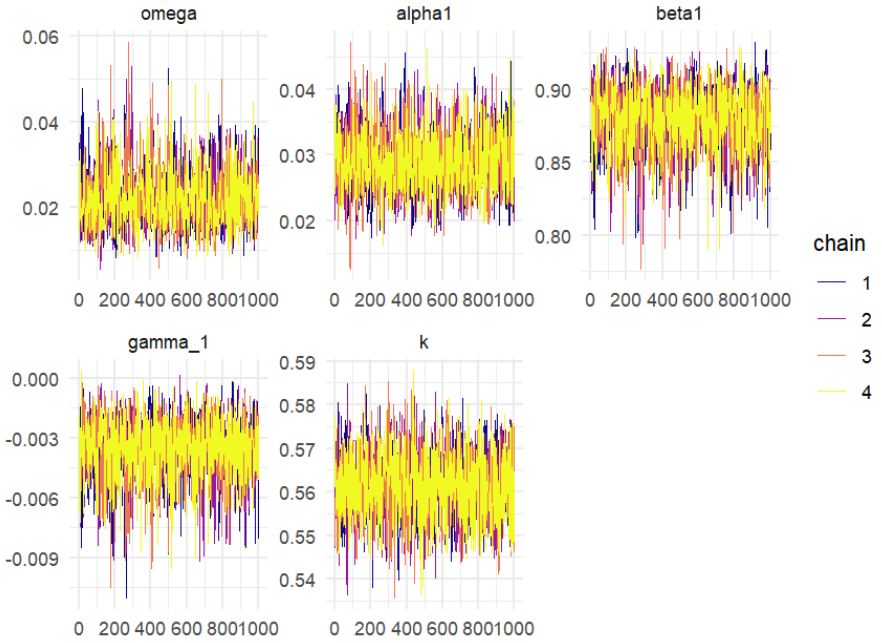

Figure 21. Trace plot of SW-ACD-X model parameters

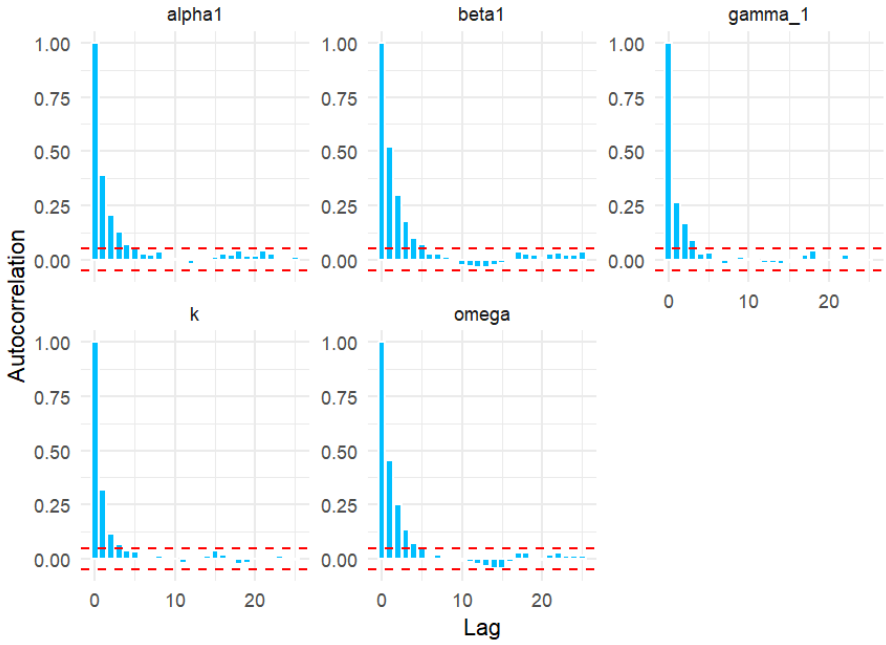

Figure 22. Autocorrelation plots of SW-ACD-X model parameters

3.2. Bayesian model selection criteria

This study utilizes a Bayesian approach to model transaction duration data, estimating model parameters based on suitably defined prior distributions. We perform a comprehensive comparative analysis of five Autoregressive conditional duration specifications: W–ACD–X, LW–ACD–X , G–ACD–X, Lomax–ACD–X, and the newly introduced SW–ACD–X model.

To assess model adequacy and predictive capability, we calculate the LOOIC using posterior samples derived from Stan. As noted by [13], LOOIC serves as a robust metric for Bayesian model selection. Additionally, in line with the suggestions of [14], we also compute the WAIC to further validate the LOOIC findings.

The most efficient model in this model selection framework is the one with the lowest information criterion values. The SW–ACD–X consistently achieves the lowest LOOIC and WAIC scores when compared to the other models, according to the empirical data, which are given in Table 9. Consequently, the SW–ACD–X model exhibits the lowest LOOIC and WAIC values, indicating that it provides the best fit for capturing the duration data when calendar effects are incorporated.

Table 9. Bayesian model selection

Model	WAIC	LOOIC
SW-ACD-X	6693.245	6693.258
Lomax -ACD-X	6706.116	6706.127
W-ACD-X	6736.272	6736.286
LW-ACD-X	6729.241	6729.25
G- ACD-X	6867.873	6867.89

4. Conclusion

The empirical findings of this study provide a promising case for the adoption of the SW–ACD–X framework in high-frequency financial modeling. By synthesizing advances in trigonometric distribution theory with the Autoregressive Conditional Duration structure, this model seeks to bridge the gap between statistical flexibility and econometric tractability. Our analysis indicates that the framework offers several advantages over traditional duration models, serving as a robust tool for capturing the complex dynamics of irregularly spaced transaction data.

The performance of the model is rooted in the flexibility of the Secant-Weibull innovation distribution. While standard ACD models, such as the Weibull–ACD, are typically restricted by monotonic hazard functions, the SW–ACD–X inherits the ability to capture non-monotonic conditional intensities. The visual and statistical evidence suggests that the secant-transformed Weibull effectively accommodates unimodal and bathtub-shaped intensities. In a market context, the bathtub-shaped trajectory is particularly relevant; it suggests that during extended periods without transactions, the probability of a trade occurring may decrease a phenomenon frequently associated with "stale" market conditions or periods of low liquidity.

Furthermore, the endogenous treatment of calendar effects represents an integrated methodological approach. While traditional two-step filtering procedures often assume independence between intraday seasonality and stochastic duration dynamics, our joint estimation strategy suggests these components are interlinked. By estimating the calendar-effect coefficients (γ_1) simultaneously with the Autoregressive parameters (α_1, β_1), the SW–ACD–X seeks to capture the interaction between deterministic diurnal patterns and stochastic clustering, providing a unified representation of the data-generating process.

From a statistical standpoint, the consistency between the Frequentist (MLE) and Bayesian (HMC–NUTS) results supports the numerical stability of the framework. In the reported IBM application, the SW–ACD–X model shows promising fit advantages as demonstrated by the AIC, BIC, WAIC, and LOOIC scores. The improvement in these information criteria over established benchmarks suggests that the added complexity of the secant transformation and exogenous variables is justified by the gain in model fit and statistical adequacy.

Our findings, supported by Monte Carlo simulations and empirical application, demonstrate the potential of the Bayesian HMC–NUTS sampler for this class of models. While the SW–ACD–X offers a robust framework for liquidity analysis, additional validation across diverse assets and market conditions is necessary to establish its broad practical superiority for trading and risk management. Future research may extend this

framework to a multivariate context to explore the co-dependencies of durations across multiple assets, or incorporate volatility duration interactions to further refine our understanding of market microstructure dynamics.

References

[1] Karam, A. (2025). Modern market microstructure liquidity, volatility and financial stability. *Volatility and Financial Stability*. https://papers.ssrn.com/sol3/papers.cfm?abstract_id=5333565&__cf_chl_rt_tk=cw3urWF7W3B8V2IvCp0WPX_8aubKNeiq3iaDMem1Q9E-1777646901-1.0.1.1-azO1QZUx._f154fhydlOB1InNSPSMNTP_7aJfTarXPs

[2] Cortese, F., et al. (2024). *Statistical Modeling and Temporal Clustering of Multivariate Time-series with Applications to Financial Data*. Università degli Studi di Milano-Bicocca.

[3] Engle, R. F., & Russell, J. R. (1998). Autoregressive conditional duration: A new model for irregularly spaced transaction data. *Econometrica*, 1127–1162.

[4] Bhogal, S. K., & Thekke Variyam, R. (2019). Conditional duration models for high-frequency data: A review on recent developments. *Journal of Economic Surveys, 33*(1), 252–273.

[5] Millat-Martinez, P., Gharbharan, A., Alemany, A., Rokx, C., Geurtsvankessel, C., Papageourgiou, G., van Geloven, N., Jordans, C., Groeneveld, G., Swaneveld, F., et al. (2021). Convalescent plasma for outpatients with early COVID-19. *medRxiv*, 2021–11.

[6] Alkhairy, I., Nagy, M., Muse, A. H., & Hussam, E. (2021). The Arctan-X family of distributions: Properties, simulation, and applications to actuarial sciences. *Complexity, 2021*(1), 4689010.

[7] Saadoon, N., Salman, H., Az-Zo'bi, E., Tashtoush, M., et al. (2025). Survival modelling of breast and brain cancer using statistical maximum likelihood and SVM techniques. *Statistics, Optimization & Information Computing*.

[8] Yan, X. (2021). Autoregressive conditional duration modelling of high frequency data. *arXiv preprint arXiv:2111.02300*.

[9] Yatigammana, R. P., Chan, J. S. K., & Gerlach, R. H. (2019). Forecasting trade durations via ACD models with mixture distributions. *Quantitative Finance, 19*(12), 2051–2067.

[10] Souza, L., de Oliveira, W. R., de Brito, C. C. R., Chesneau, C., Fernandes, R., & Ferreira, T. A. E. (2022). Sec-G class of distributions: Properties and applications. *Symmetry, 14*(2), 299.

[11] Van de Schoot, R., Depaoli, S., King, R., Kramer, B., Märtens, K., Tadesse, M. G., Vannucci, M., Gelman, A., Veen, D., Willemsen, J., et al. (2021). Bayesian statistics and modelling. *Nature Reviews Methods Primers, 1*(1), 1.

[12] Leigh, G. M., & Northrop, A. R. (2022). Design of Hamiltonian Monte Carlo for perfect simulation of general continuous distributions. *arXiv preprint arXiv:2212.12140*.

[13] Gelman, A., & Rubin, D. B. (1995). Avoiding model selection in Bayesian social research. *Sociological Methodology, 25*, 165–173.

[14] Gelman, A., Hwang, J., & Vehtari, A. (2014). Understanding predictive information criteria for Bayesian models. *Statistics and Computing, 24*(6), 997–1016.